

On Implicit Filter Level Sparsity in Convolutional Neural Networks

Dushyant Mehta^[1,3], Kwang In Kim^[2], Christian Theobalt^[1,3]

[1] MPI For Informatics [2] University of Bath [3] Saarland Informatics Campus

Abstract

We investigate filter level sparsity that emerges in convolutional neural networks (CNNs) which employ Batch Normalization and ReLU activation, and are trained with adaptive gradient descent techniques and L2 regularization (or weight decay). We conduct an extensive experimental study casting these initial findings into hypotheses and conclusions about the mechanisms underlying the emergent filter level sparsity. This study allows new insight into the performance gap observed between adaptive and non-adaptive gradient descent methods in practice. Further, analysis of the effect of training strategies and hyperparameters on the sparsity leads to practical suggestions in designing CNN training strategies enabling us to explore the tradeoffs between feature selectivity, network capacity, and generalization performance. Lastly, we show that the implicit sparsity can be harnessed for neural network speedup at par or better than explicit sparsification / pruning approaches, without needing any modifications to the typical training pipeline.

1. Introduction

In this work we show that filter¹ level sparsity emerges in certain types of feedforward convolutional neural networks. In networks which employ Batch Normalization and ReLU activation, after training, certain filters are observed to not activate for any input. We investigate the cause and implications of this emergent sparsity. Our findings relate to the anecdotally known and poorly understood ‘dying ReLU’ phenomenon [1], wherein some features in ReLU networks get cut off while training, leading to a reduced effective learning capacity of the network. Approaches such as Leaky ReLU [22] and RandomOut [3] propose symptomatic fixes but with a limited understanding of the cause.

We conclude, through a systematic experimental study, that the emergence of sparsity is the direct result of a disproportionate relative influence of the regularizer (L2 or weight

¹Filter refers to the weights and the nonlinearity associated with a particular feature, acting together as a unit. We use filter and feature interchangeably throughout the document.

decay) viz a viz the gradients from the primary training objective of ReLU networks.

The extent of the resulting sparsity is affected by multiple phenomena which subtly impact the relative influence of the regularizer. Many of the hyperparameters and design choices for training neural networks interplay with these phenomena to influence the extent of sparsity. We show that increasing the mini-batch size decreases the extent of sparsity, adaptive gradient descent methods exhibit a much higher sparsity than stochastic gradient descent (SGD) for both L2 regularization and weight decay, and L2 regularization couples with adaptive gradient methods to further increase sparsity compared to weight decay.

We show that understanding the impact of these design choices yields useful and readily controllable sparsity which can be leveraged for considerable neural network speed up, without trading the generalization performance and without requiring any explicit pruning [23, 18] or sparsification [19] steps. The implicit sparsification process can remove 70-80% of the convolutional filters from VGG-16 on CIFAR10/100, far exceeding that for [18], and performs comparable to [19] for VGG-11 on ImageNet.

Further, the improved understanding of the sparsification process we provide can better guide efforts towards developing strategies for ameliorating its undesirable aspects, while retaining the desirable properties. Also, our insights will lead practitioners to be more aware of the implicit tradeoffs between network capacity and generalization being made underneath the surface, while changing hyperparameters seemingly unrelated to network capacity.

2. Emergence of Filter Sparsity in CNNs

2.1. Setup and Preliminaries

Our basic setup is comprised of a 7-layer convolutional network with 2 fully connected layers as shown in Figure 1. The network structure is inspired by VGG [28], but is more compact. We refer to this network as *BasicNet* in the rest of the document. We use a variety of gradient descent approaches, a batch size of 40, with a method specific base learning rate for 250 epochs, and scale down the learning rate by 10 for an additional 75 epochs. We train on CIFAR10 and CIFAR 100 [16], with normalized images,

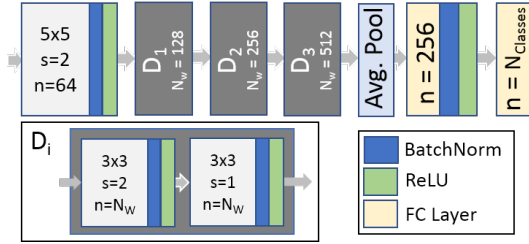


Figure 1. **BasicNet**: Structure of the basic convolution network studied in this paper. We refer to the individual convolution layers as C1-7. The fully connected head shown here is for CIFAR10/100, and a different fully-connected structure is used for TinyImageNet and ImageNet.

and random horizontal flips used while training. Xavier initialization [7] is used for the network weights, with the appropriate gain for ReLU. The base learning rates and other hyperparameters are as follows: Adam (1e-3, $\beta_1=0.9$, $\beta_2=0.99$, $\epsilon=1e-8$), Adadelta (1.0, $\rho=0.9$, $\epsilon=1e-6$), SGD (0.1, momentum=0.9), Adagrad (1e-2). Pytorch [26] is used for training, and we study the effect of varying the amount and type of regularization on the extent of sparsity and test error in Table 1. **L2 regularization vs. Weight Decay**: We make a distinction between L2 regularization and weight decay. For a parameter θ and regularization hyperparameter $1 > \lambda \geq 0$, weight decay multiplies θ by $(1 - \lambda)$ after the update step based on the gradient from the main objective. While for L2 regularization, $\lambda\theta$ is added to the gradient $\nabla L(\theta)$ from the main objective, and the update step is computed using this sum. See [21] for a detailed discussion.

Quantifying Feature Sparsity: We measure the learned feature sparsity in two ways, by per-feature activation and by per-feature scale. For sparsity by activation, for each feature we apply max pooling to the absolute activations over the entire feature plane, and consider the feature inactive if this value does not exceed 10^{-12} over the entire *training* corpus. For sparsity by scale, we consider the scale γ of the learned affine transform in the Batch Norm [12] layer. Batch normalization uses additional learned scale γ and bias β that casts each normalized convolution output \hat{x}_i to $y_i = \gamma\hat{x}_i + \beta$. We consider a feature inactive if $|\gamma|$ for the feature is less than 10^{-3} . Explicitly zeroing the features thus marked inactive does not affect the test error, which ensures the validity of our chosen thresholds. The thresholds chosen are purposefully conservative, and comparable levels of sparsity are observed for a higher feature activation threshold of 10^{-4} , and a higher $|\gamma|$ threshold of 10^{-2} .

2.2. Primary Findings

Table 1 shows the overall feature sparsity by activation (Act.) and by scale (γ) for BasicNet. Only convolution features are considered. The following are the key observations from the experiments and the questions they raise. These are further discussed in Section 2.3.

Table 1. Convolutional filter sparsity in *BasicNet* trained on CIFAR10/100 for different combinations of regularization and gradient descent methods. Shown are the % of non-useful / inactive convolution filters, as measured by activation over training corpus (max act. $< 10^{-12}$) and by the learned BatchNorm scale ($|\gamma| < 10^{-03}$), averaged over 3 runs. The lowest test error per optimizer is highlighted, and sparsity (green) or lack of sparsity (red) for the best and near best configurations indicated via text color. L2: L2 regularization, WD: Weight decay (adjusted with the same scaling schedule as the learning rate schedule).

	L2	CIFAR10			CIFAR100		
		% Sparsity by Act	% Sparsity by γ	Test Error	% Sparsity by Act	% Sparsity by γ	Test Error
SGD	2e-03	54	54	30.9	69	69	64.8
	1e-03	27	27	21.8	23	23	47.1
	5e-04	9	9	16.3	4	4	42.1
	2e-04	0	0	13.1	0	0	38.8
	1e-04	0	0	11.8	0	0	37.4
	1e-05	0	0	10.5	0	0	39.0
	0	0	0	11.3	0	0	40.1
Adam [15]	1e-02	82	85	21.3	87	85	69.7
	2e-03	88	86	14.7	82	81	42.7
	1e-03	85	83	13.1	77	76	39.0
	1e-04	71	70	10.5	47	47	36.6
	1e-05	48	48	10.7	5	5	40.6
	1e-06	24	24	10.9	0	0	40.5
	0	3	0	11.0	0	0	40.3
Adadelta [32]	1e-02	97	97	36.8	98	98	84.1
	2e-03	92	92	20.6	89	89	53.2
	1e-03	89	89	16.7	82	82	46.3
	5e-04	82	82	13.6	61	61	39.1
	2e-04	40	40	11.3	3	3	35.4
1e-04	1	1	10.2	1	1	35.9	
Adagrad [6]	2e-02	75	75	11.3	88	88	63.3
	1e-02	65	65	11.2	59	59	37.2
	5e-03	56	56	11.3	24	25	35.9
	1e-03	27	28	11.9	1	1	37.3
	1e-04	0	0	13.6	0	0	42.1
SGD		CIFAR10			CIFAR100		
		% Sparsity by Act	% Sparsity by γ	Test Error	% Sparsity by Act	% Sparsity by γ	Test Error
	1e-02	100	100	90.0	100	100	99.0
	1e-03	27	27	21.6	23	23	47.6
	5e-04	8	8	15.8	4	4	41.9
	2e-04	0	0	13.3	0	0	39.4
	1e-04	0	0	12.4	0	0	37.7
Adam [15]	1e-02	100	100	82.3	100	100	98.0
	1e-03	90	90	27.8	81	81	55.3
	5e-04	81	81	18.1	59	59	43.3
	2e-04	60	60	13.4	16	16	37.3
	1e-04	40	40	11.2	3	3	36.2

1): The emergent sparsity relies on the strength of L2

Table 2. Layerwise % filters pruned from BasicNet trained on CIFAR100, based on the $|\gamma| < 10^{-3}$ criteria. Also shown are pre-pruning and post-pruning test error, and the % of *convolutional* parameters pruned. C1-C7 indicate Convolution layer 1-7, and the numbers in parantheses indicate the total number of features per layer. Average of 3 runs. Refer to the supplementary document for the corresponding table for CIFAR10.

		Train Loss	Test Loss	Test Err	% Sparsity by γ or % Filters Pruned							% Param		
					C1 (64)	C2 (128)	C3 (128)	C4 (256)	C5 (256)	C6 (512)	C7 (512)	Total (1856)	Pruned (4649664)	Pruned Test Err.
Adam	L2: 1e-3	1.06	1.41	39.0	56	47	43	68	72	91	85	76	95	39.3
	L2: 1e-4	0.10	1.98	36.6	41	20	9	33	34	67	55	46	74	36.6
	WD: 2e-4	0.34	1.56	37.3	55	20	3	4	2	16	26	16	27	37.3
	WD: 1e-4	0.08	1.76	36.2	38	4	0	0	0	0	5	3	4	36.2
SGD	L2: 1e-3	1.49	1.78	47.1	82	41	33	29	33	6	18	23	34	47.1
	L2: 5e-4	0.89	1.69	42.1	64	3	3	3	2	0	2	4	4	42.1
	WD: 1e-3	1.49	1.79	47.6	82	43	31	28	33	6	17	23	34	47.6
	WD: 5e-4	0.89	1.69	41.9	66	2	1	4	2	0	1	4	4	41.9

regularization or weight decay. **No sparsity is observed in the absence of regularization, with sparsity increasing with increasing L2 or weight decay.** *What does this tell us about the cause of sparsification, and how does the sparsity manifest across layers?*

2): Regardless of the type of regularizer (L2 or weight decay), **adaptive methods (Adam, Adagrad, Adadelta) learn sparser representations than SGD for comparable levels of test error**, with Adam showing the most sparsity and most sensitivity to the L2 regularization parameter amongst the ones studied. Adam with L2 sees about 70% features pruned for CIFAR10, while SGD shows no sparsity for a comparable performance, with a similar trend for CIFAR100, as well as when weight decay is used. *What are the causes for this disparity in sparsity between SGD and adaptive methods?* We will focus on understanding the disparity between SGD and Adam.

3): SGD has comparable levels of sparsity with L2 regularization and with weight decay (for higher regularization values), while **for Adam, L2 shows higher sparsity for comparable performance than weight decay** (70% vs 40% on CIFAR10, 47% vs 3% on CIFAR100). *Why is there a significant difference between the sparsity for Adam with L2 regularization vs weight decay?*

4): The extent of sparsity decreases on moving from the simple 10 class classification problem of CIFAR10 to the comparatively harder 100 class classification problem of CIFAR100. *What does the task dependence of the extent of sparsity tell us about the origin of the sparsity?*

2.3. A Detailed Look at The Emergent Sparsity

The analysis of Table 1 in the preceding section shows that the regularizer (L2 or weight decay) is very likely the cause of the sparsity, with differences in the level of sparsity attributable to the particular interaction of L2 regularizer (and lack of interaction of weight decay) with the update mechanism. The differences between adaptive gradient methods (Adam) and SGD can additionally likely be

attributed to differences in the nature of the learned representations between the two. That would explain the higher sparsity seen for Adam in the case of weight decay.

Layer-wise Sparsity: To explore the role of the regularizer in the sparsification process, we start with a layer-wise breakdown of sparsity. For each of Adam and SGD, we consider both L2 regularization and weight decay in Table 2 for CIFAR100. The table shows sparsity by scale ($|\gamma| < 10^{-3}$) for each convolution layer. For both optimizer-regularizer pairings we pick the configurations from Table 1 with the lowest test errors that also produce sparse features. For SGD, the extent of sparsity is higher for earlier layers, and decreases for later layers. The trend holds for both L2 and weight decay, from C1-C6. Note that the higher sparsity seen for C7 might be due to its interaction with the fully connected layers that follow. Sparsity for Adam shows a similar decreasing trend from early to middle layers, and increasing sparsity from middle to later layers.

Surprising Similarities to Explicit Feature Sparsification: In the case of Adam, the trend of layerwise sparsity exhibited is similar to that seen in explicit feature sparsification approaches (See Table 8 in [20] for Network Slimming [19]). If we explicitly prune out features meeting the $|\gamma| < 10^{-3}$ sparsity criteria, we still see a relatively high performance on the test set even with 90% of the convolutional parameters pruned. Network Slimming [19] uses explicit sparsity constraints on BatchNorm scales (γ). The similarity in the trend of Adam’s emergent layer-wise sparsity to that of explicit scale sparsification motivates us to examine the distribution of the learned scales (γ) and biases (β) of the BatchNorm layer in our network. We consider layer C6, and in Figure 2 show the evolution of the distribution of the learned bias and scales as training progresses on CIFAR100. We consider a low L2 regularization value of 1e-5 and a higher L2 regularization value of 1e-4 for Adam, and also show the same for SGD with L2 regularization of 5e-4. The lower regularization values, which do not induce sparsity, would help shed light at the underlying processes

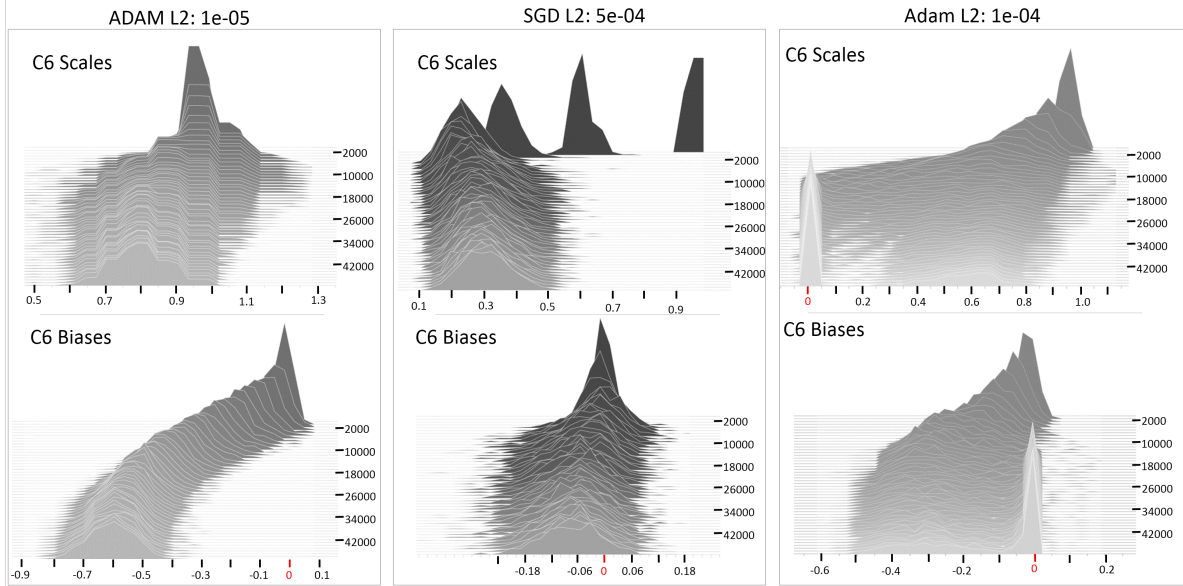


Figure 2. **Emergence of Feature Selectivity with Adam** The evolution of the learned scales (γ , top row) and biases (β , bottom row) for layer C6 of *BasicNet* for Adam and SGD as training progresses. Adam has distinctly negative biases, while SGD sees both positive and negative biases. For positive scale values, as seen for both Adam and SGD, this translates to greater feature selectivity in the case of Adam, which translates to a higher degree of sparsification when stronger regularization is used. Note the similarity of the final scale distribution for Adam L2:1e-4 to the scale distributions shown in Figure 4 in [19]

without interference from the sparsification process.

Feature Selectivity Hypothesis: From Figure 2 the differences between the nature of features learned by Adam and SGD become clearer. For zero mean, unit variance BatchNorm outputs $\{\hat{x}_i\}_{i=1}^N$ of a particular convolutional kernel, where N is the size of the training corpus, due to the use of ReLU, a gradient is only seen for those datapoints for which $\hat{x}_i > -\beta/\gamma$. Both SGD and Adam (L2: 1e-5) learn positive γ s for layer C6, however β s are negative for Adam, while for SGD some of the biases are positive. This implies that all features learned for Adam (L2: 1e-5) in this layer activate for \leq half the activations from the training corpus, while SGD has a significant number of features activate for more than half of the training corpus, i.e., Adam learns more selective features in this layer. Features which activate only for a small subset of the training corpus, and consequently see gradient updates from the main objective less frequently, continue to be acted upon by the regularizer. If the regularization is strong enough (Adam with L2: 1e-4 in Fig. 2), or the gradient updates infrequent enough (feature too selective), the feature may be pruned away entirely. The propensity of later layers to learn more selective features with Adam would explain the higher degree of sparsity seen for later layers as compared to SGD.

Quantifying Feature Selectivity: Similar to feature sparsity by activation, we apply max pooling to a feature’s absolute activations over the entire feature plane. For a particular feature, we consider these pooled activations over the entire training corpus and normalize them by the max of the

pooled activations over the entire training corpus. We then consider the percentage of the training corpus for which this normalized pooled value exceeds a threshold of 10^{-3} . We refer to this percentage as the feature’s *universality*. A feature’s selectivity is then defined as $100 - \text{universality}$. Unlike the selectivity metrics employed in literature [24], ours is class agnostic. In Figure 3, we compare the ‘universality’ of features learned with Adam and SGD per layer on CIFAR100, for both low and higher regularization values. For the low regularization case, we see that in C6 and C7 both Adam and SGD learn selective features, with Adam showing visibly ‘more selectivity for C6 (blue bars shifted left)’. The disproportionately stronger regularization effect of L2 coupled with Adam becomes clearer when moving to a higher regularization value. The selectivity for SGD in C6 remains mostly unaffected, while Adam sees a large fraction (64%) of the features inactivated (0% universality). Similarly for C7, the selectivity pattern remains the same on moving from lower regularization to higher regularization, but Adam sees more severe feature inactivation.

Interaction of L2 Regularizer with Adam: Next, we consider the role of the L2 regularizer vs. weight decay. We study the behaviour of L2 regularization in the low gradient regime for different optimizers. Figure 4 shows that coupling of L2 regularization with ADAM update equation yields a faster decay than weight decay, or L2 regularization with SGD, even for smaller regularizer values. This is an additional source of regularization disparity between parameters which see frequent updates and those which don’t

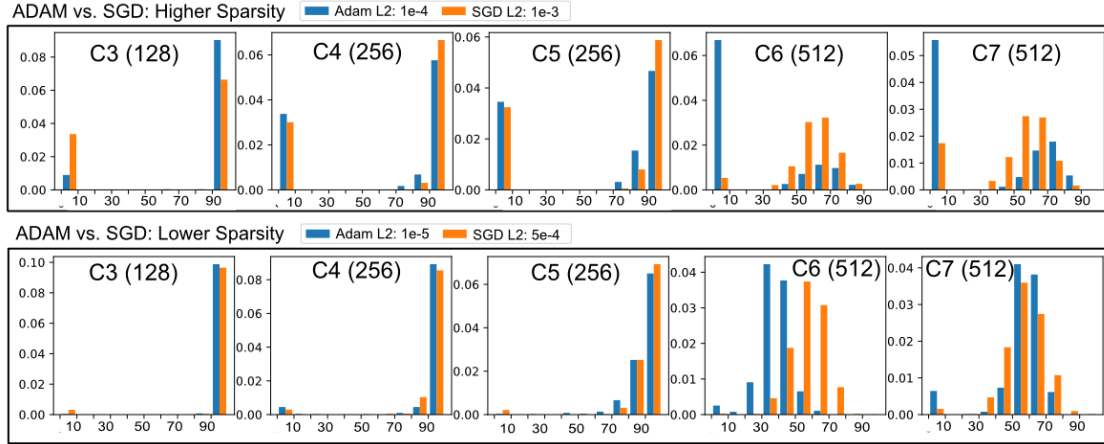


Figure 3. **Layer-wise Feature Selectivity** Feature universality for CIFAR 100, with Adam and SGD. X-axis shows the universality and Y-axis ($\times 10$) shows the fraction of features with that level of universality. For later layers, Adam tends to learn less universal features than SGD, which get pruned by the regularizer. Please be mindful of the differences in Y-axis scales between plots. Refer to the supplementary document for a similar analysis for CIFAR10

see frequent updates or see lower magnitude gradients. It manifests for certain adaptive gradient descent approaches.

3. Related Work

Effect of L2 regularization vs. Weight Decay for Adam: Prior work [21] has indicated that Adam with L2 regularization leads to parameters with frequent and/or large magnitude gradients from the main objective being regularized less than the ones which see infrequent and/or small magnitude gradients. Though weight decay is proposed as a supposed fix, we show that there are rather two different aspects to consider. The first is the disparity in effective regularization due to the frequency of updates. Parameters which update less frequently would see more regularization steps per actual update than those which are updated more frequently. This disparity would persist even with weight decay due to Adam’s propensity for learning more selective features, as detailed in the preceding section. The second aspect is the additional disparity in regularization for features which see low/infrequent gradient, due to the coupling of L2 regularization with Adam.

Attributes of Generalizable Neural Network Features: Dinh et al. [5] show that the geometry of minima is not invariant to reparameterization, and thus the flatness of the minima may not be indicative of generalization performance [13], or may require other metrics which are invariant to reparameterization. Morcos et al. [24] suggest based on extensive experimental evaluation that good generalization ability is linked to reduced selectivity of learned features. They further suggest that individual selective units do not play a strong role in the overall performance on the task as compared to the less selective ones. They connect the ablation of selective features to the heuristics employed in neural network feature pruning literature which prune

features whose removal does not impact the overall accuracy significantly [23, 18]. The findings of Zhou et al. [33] concur regarding the link between emergence of feature selectivity and poor generalization performance. They further show that ablation of class specific features does not influence the overall accuracy significantly, however the specific class may suffer significantly. We show that the emergence of selective features in Adam, and the increased propensity for pruning the said selective features when using L2 regularization presents a direct tradeoff between generalization performance and network capacity which practitioners using Adam must be aware of.

Observations on Adaptive Gradient Descent: Several works have noted the poorer generalization performance of adaptive gradient descent approaches over SGD. Keskar et al. [14] propose to leverage the faster initial convergence of ADAM and the better generalization performance of SGD, by switching from ADAM to SGD while training. Reddi et al. [27] point out that exponential moving average of past squared gradients, which is used for all adaptive gradient approaches, is problematic for convergence, particularly with features which see infrequent updates. This short term memory is likely the cause of accelerated pruning of selective features seen for Adam in Figure 4 (and other adaptive gradient approaches), and the extent of sparsity observed would be expected to go down with AMSGrad which tracks the long term history of squared gradients.

Heuristics for Feature Pruning/Sparsification:

We give a brief overview of filter and weight pruning approaches, focusing on the various heuristics proposed for gauging synaptic (weights) and neuronal (filter) importance. Synaptic importance heuristics range from crude measures such as parameter magnitudes [8, 10] to more sophisticated and expensive to compute second order estimates [17, 9]. On the other hand neuronal importance ap-

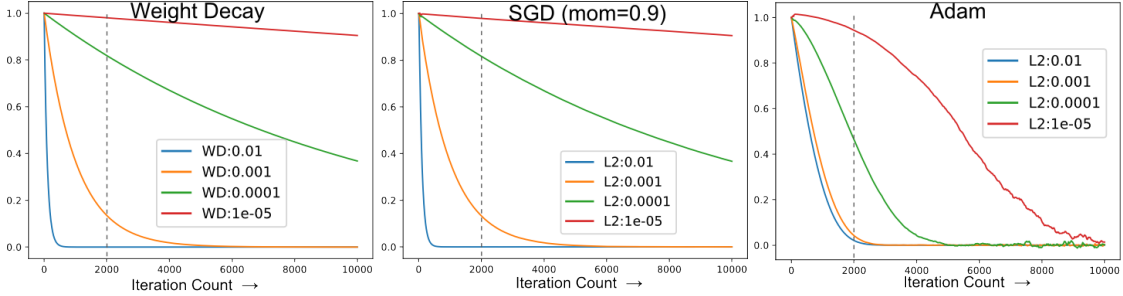


Figure 4. The action of regularization on a scalar value, for a range of regularization values in the presence of simulated low gradients drawn from a mean=0, $\text{std}=10^{-5}$ normal distribution. The gradients for the first 100 iterations are drawn from a mean=0, $\text{std}=10^{-3}$ normal distribution to emulate a transition into low gradient regime rather than directly starting in a low gradient regime. The learning rate for SGD(momentum=0.9) is 0.1, and the learning rate for ADAM is 1e-3. We show similar plots for other adaptive gradient descent approaches in the supplementary document.

proaches for post-hoc pruning remove whole features instead of individual parameters, and are more amenable to acceleration on existing hardware. The filter importance heuristics employed for these include weight norm of a filter [18, 29], the average percentage of zero outputs of a node over the dataset [11], feature saliency based on first [23, 25] and second order [30] Taylor expansion of the loss or a surrogate [25]. The feature computation cost can also be included in the pruning objective [23, 30].

Various approaches [31, 19] make use of the learned scale parameter γ in Batch Norm for enforcing sparsity on the filters. Ye et al. [31] argue that BatchNorm makes feature importance less susceptible to scaling reparameterization, and the learned scale parameters (γ) can be used as indicators of feature importance. We find that Adam with L2 regularization, owing to its implicit pruning of features based on feature selectivity, makes it an attractive alternative to explicit sparsification/pruning approaches. The link between ablation of selective features and explicit feature pruning is also established in prior work [24, 33].

4. Further Experiments

We conduct additional experiments on additional datasets and various different network architectures to show that the intuition developed in the preceding sections generalizes. Further, we provide additional support by analysing the effect of various hyperparameters on the extent of sparsity. We also compare the emergent sparsity for different networks on various datasets to that of explicit sparsification approaches [18, 19].

Datasets: In addition to CIFAR10 and CIFAR100, we also consider TinyImageNet [2] which is a 200 class subset of ImageNet [4] with images resized to 64×64 pixels. The same training augmentation scheme is used for TinyImageNet as for CIFAR10/100. We also conduct extensive experiments on ImageNet. The images are resized to 256×256 pixels, and random crops of size 224×224 pixels, used while training, combined with random horizontal flips.

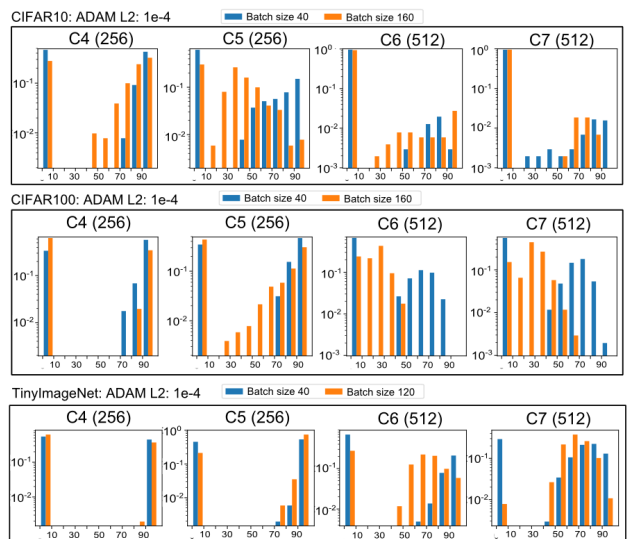


Figure 5. **Feature Selectivity For Different Mini-Batch Sizes for Different Datasets** Feature universality ($1 - \text{selectivity}$) plotted for layers C4-C7 of *BasicNet* for CIFAR10, CIFAR100 and TinyImageNet. Batch sizes of 40/160 considered for CIFAR, and 40/120 for TinyImageNet.

For testing, no augmentation is used, and 1-crop evaluation protocol is followed.

Network Architectures: The convolution structure for *BasicNet* stays the same across tasks, while the fully-connected (fc) structure changes across task. We will use ‘[n]’ to indicate an fc layer with n nodes. Batch Norm and ReLU are used in between fc layers. For CIFAR10/100 we use Global Average Pooling (GAP) after the last convolution layer and the fc structure is $[256][10]/[256][100]$, as shown in Figure 1. For TinyImageNet we again use GAP followed by $[512][256][200]$. On ImageNet we use average pooling with a kernel size of 5 and a stride of 4, followed by $[4096][2048][1000]$. For VGG-11/16, on CIFAR10/100 we use $[512][10]/[512][100]$. For TinyImageNet we use $[512][256][200]$, and for ImageNet we use the structure in [28]. For VGG-19, on CIFAR10/100, we use an fc struc-

ture identical to [19]. Unless explicitly stated, we will be using Adam with L2 regularization of $1e-4$, and a batch size of 40. When comparing different batch sizes, we ensure the same number of training iterations.

4.1. Analysis of Hyperparameters

Having established in Section 2.3 (Figures 3 and 2) that with Adam, the emergence of sparsity is correlated with feature selectivity, we investigate the impact of various hyperparameters on the emergent sparsity.

Effect of Mini-Batch Size: Figure 5 shows the extent of feature selectivity for C4-C7 of *BasicNet* on CIFAR and TinyImageNet for different mini-batch sizes. For each dataset, note the apparent increase in selective features with increasing batch size. However, a larger mini-batch size is not promoting feature selectivity, and rather preventing the selective features from being pruned away by providing more frequent updates. This makes the mini-batch size a key knob to control tradeoffs between network capacity (how many features get pruned, which affects the speed and performance) and generalization ability (how many selective features are kept, which can be used to control overfitting). We see across datasets and networks that increasing the mini-batch size leads to a decrease in sparsity (Tables 3, 5, 6, 7, 8, 9, 10).

The difficulty of the task vs. the capacity of the network directly impact the emergence of selective features (Figure 5), and thus will influence the sparsity.

Network Capacity: We also consider variations of *BasicNet* in Table 4 to study the effect of network capacity. We indicate the architecture presented in Figure 1 as ‘64-1x’, and consider two variants: ‘64-0.5x’ which has 64 features in the first convolution layer, and half the features of *BasicNet* in the remaining convolution layers, and ‘32-0.25x’ with 32 features in the first channel and a quarter of the features in the remaining layers. The fc-head remains unchanged. We see a consistent decrease in the extent of sparsity with decreasing network width in Table 4. Additionally note the decrease in sparsity in moving from CIFAR10 to CIFAR100.

Increasing Task ‘Difficulty’: As the task becomes more difficult, for a given network capacity, we expect the fraction of features pruned to decrease corresponding to a decrease in selectivity of the learned features [33]. This is indeed observed in Table 1 for *BasicNet* for all gradient descent methods on moving from CIFAR10 to CIFAR100. For Adam with L2 regularization, 70% sparsity on CIFAR 10 decreases to 47% on CIFAR 100, and completely vanishes on ImageNet (See Table 6). Similarly, for VGG-16, the sparsity goes from $>80\%$ on CIFAR-10 to 70% on CIFAR 100 in Table 7, to 61% for TinyImageNet and 7% for ImageNet in Table 8. Figure 5 shows the extent of feature selectivity for C4-C7 of *BasicNet* on CIFAR and TinyIma-

geNet. Note the distinct shift towards more universal features as the task difficulty increases. Also note that SGD shows no sparsity at all for TinyImageNet (Table 5).

Table 3. BasicNet sparsity variation on CIFAR10/100 trained with Adam and L2 regularization.

		CIFAR 10				CIFAR 100			
	Batch Size	Train Loss	Test Loss	Test Err	%Spar. by γ	Train Loss	Test Loss	Test Err	%Spar. by γ
L2: $1e-3$	20	0.43	0.45	15.2	82	1.62	1.63	45.3	79
	40	0.29	0.41	13.1	83	1.06	1.41	39.0	76
	80	0.18	0.40	12.2	80	0.53	1.48	37.1	67
L2: $1e-4$	20	0.17	0.36	11.1	70	0.69	1.39	35.2	57
	40	0.06	0.43	10.5	70	0.10	1.98	36.6	46
	80	0.02	0.50	10.1	66	0.02	2.21	41.1	35
	160	0.01	0.55	10.6	61	0.01	2.32	44.3	29

Table 4. Effect of varying the number of features in BasicNet.

Net Cfg.	CIFAR 10				CIFAR 100			
	Train Loss	Test Loss	Test Err	%Spar. by γ	Train Loss	Test Loss	Test Err	%Spar. by γ
64-1x	0.06	0.43	10.5	70	0.10	1.98	36.6	46
64-0.5x	0.10	0.41	11.0	51	0.11	2.19	39.8	10
32-0.25x	0.22	0.44	13.4	23	0.51	2.05	43.4	0

Table 5. Convolutional filter sparsity for BasicNet trained on TinyImageNet, with different mini-batch sizes.

	Batch Size	Train Loss	Val Loss	Top 1 Val Err.	Top 5 Val Err.	% Spar. by γ
SGD	40	0.02	2.63	45.0	22.7	0
	20	1.05	2.13	47.7	22.8	63
Adam	40	0.16	2.96	48.4	24.7	48
	120	0.01	2.48	48.8	27.4	26

Table 6. Convolutional filter sparsity of BasicNet on ImageNet.

Batch Size	Train Loss	Val Loss	Top 1 Val Err.	Top 5 Val Err.	% Sparsity by γ
64	2.05	1.58	38.0	15.9	0.2
256	1.63	1.35	32.9	12.5	0.0

4.2. Comparison With Explicit Feature Sparsification / Pruning Approaches

For VGG-16, we compare the network trained on CIFAR-10 with Adam using different mini-batch sizes against the handcrafted approach of Li et al. [18]. Similar to tuning the explicit sparsification hyperparameter in [19], the mini-batch size can be varied to find the sparsest representation with an acceptable level of test performance. We see from Table 7 that when trained with a batch size of 160, 83% of the features can be pruned away and leads to a better performance than the 37% of the features pruned for [18]. For VGG-11 on ImageNet (Table 9), by simply varying the mini-batch size from 90 to 60, the number of convolutional

features pruned goes from 71 to 140. This is in the same range as the number of features pruned by the explicit sparsification approach of [18], and gives a comparable top-1 and top-5 validation error. For VGG-19 on CIFAR10 and CIFAR100 (Table 10), we see again that varying the mini-batch size controls the extent of sparsity. For the mini-batch sizes we considered, the extent of sparsity is much higher than that of [19], with consequently slightly worse performance. The mini-batch size or other hyper-parameters can be tweaked to further tradeoff sparsity for accuracy, and reach a comparable sparsity-accuracy point as [19].

Table 7. Layerwise % Sparsity by γ for VGG-16 on CIFAR10 and 100. Also shown is the handcrafted sparse structure of [18]

Conv Layer	#Conv Feat.	CIFAR 10				CIFAR 100		
		Adam, L2:1e-4 B: 40	B: 80	B: 160	Li et al.[18]	Adam, L2:1e-4 B: 40	B: 80	B: 160
C1	64	64	0	0	50	49	1	58
C2	64	18	0	0	0	4	0	8
C3	128	50	47	51	0	29	40	54
C4	128	12	5	6	0	0	0	3
C5	256	46	40	36	0	10	5	27
C6	256	71	66	63	0	26	5	7
C7	256	82	80	79	0	44	12	0
C8	512	95	96	96	50	86	74	55
C9	512	97	97	97	50	95	90	94
C10	512	97	97	96	50	96	93	93
C11	512	98	98	98	50	98	97	96
C12	512	99	99	98	50	98	98	99
C13	512	99	99	99	50	98	98	96
%Feat. Pruned		86	84	83	37	76	69	69
Test Err		7.2	7.0	6.5	6.6	29.2	28.1	27.8

Table 8. Sparsity by γ on VGG-16, trained on TinyImageNet, and on ImageNet. Also shown are the pre- and post-pruning top-1/top-5 single crop validation errors. Pruning using $|\gamma| < 10^{-3}$ criteria.

TinyImageNet	# Conv	Pre-pruning		Post-pruning	
	Feat. Pruned	top1	top5	top1	top5
L2: 1e-4, B: 20	3016 (71%)	45.1	21.4	45.1	21.4
L2: 1e-4, B: 40	2571 (61%)	46.7	24.4	46.7	24.4
ImageNet					
L2: 1e-4, B: 40	292	29.93	10.41	29.91	10.41

Table 9. Effect of different mini-batch sizes on sparsity (by γ) in VGG-11, trained on ImageNet. Same network structure employed as [19]. * indicates finetuning after pruning

	# Conv	Pre-pruning		Post-pruning	
	Feat. Pruned	top1	top5	top1	top5
Adam, L2: 1e-4, B: 90	71	30.50	10.65	30.47	10.64
Adam, L2: 1e-4, B: 60	140	31.76	11.53	31.73	11.51
Liu et al. [19] from [20]	85	29.16		31.38*	-

Table 10. Sparsity by γ on VGG-19, trained on CIFAR10/100. Also shown are the post-pruning test error. Compared with explicit sparsification approach of Liu et al. [19]

	CIFAR 10			CIFAR 100		
	Adam, L2:1e-4 B: 64	L2:1e-4 B: 512	Li et al.[19]	Adam, L2:1e-4 B: 64	L2:1e-4 B: 512	Li et al.[19]
%Feat. Pruned	85	81	70	75	62	50
Test Err	7.1	6.9	6.3	29.9	28.8	26.7

5. Discussion and Future Work

We point out that practitioners must be aware of the underlying inadvertent changes in network capacity as well as the tradeoffs with regards to generalization made by changing common hyperparameters such as mini-batch size when using adaptive gradient descent methods. The root cause of sparsity we reveal would continue to be an issue even when supposed fixes such as Leaky ReLU are used. We see that with *BasicNet* on CIFAR100 Leaky ReLU with a negative slope of 0.01 only marginally reduces the extent of sparsity in the case of Adam with L2: 10^{-4} (41% feature sparsity for 36.8% test error, vs. 47% feature sparsity for 36.6% test error with ReLU), but does not completely remove it. We hope that the better understanding we contribute of the mechanism of sparsification would prompt attempts at better solutions to address the harmful aspects of the emergent sparsity, while retaining the useful aspects. Additionally, though we show Adam with L2 regularization works out of the box for speeding up neural networks, it lacks some of the desirable properties of explicit sparsification approaches, such as layer computation cost aware sparsification, or being able to successively build multiple compact models out of a single round of training like in [31]. Investigating ways of incorporating these would be another possible line of work.

6. Conclusion

We demonstrate through extensive experiments that the root cause for the emergence of filter level sparsity in convolutional neural networks is the disproportionate regularization (L2 or weight decay) of the parameters in comparison to the gradient from the primary objective. We identify how various parameters influence the extent of sparsity by interacting in subtle ways with the regularization. We show that adaptive gradient updates play a crucial role in the emergent sparsity (in contrast to SGD), and Adam not only shows a higher degree of sparsity but the extent of sparsity also has a strong dependence on the mini-batch size. We show that this is caused by the propensity of Adam to learn more selective features, and the added acceleration of L2 regularization in low gradient regime.

Due to its targeting of selective features, the emergent sparsity can be used to trade off between network capacity, performance and generalization ability as per the task setting, and common hyperparameters such as mini-batch size allow direct control over it. We leverage this fine-grained control and show that Adam with L2 regularization can be an attractive alternative to explicit network slimming approaches for speeding up test time performance of convolutional neural networks, without requiring any tooling changes to the traditional neural network training pipeline supported by the existing frameworks.

Supplementary Document: On Implicit Filter Level Sparsity In Convolutional Neural Networks

In this supplemental document, we provide additional experiments that show how filter level sparsity manifests under different gradient descent flavours and regularization settings (Sec. 1), and that it even manifests with Leaky ReLU. We also show the emergence of feature selectivity in Adam in multiple layers, and discuss its implications on the extent of sparsity (Sec. 2). In Section 3 we consider additional hyperparameters that influence the emergent sparsity. In Section 4 we provide specifics for some of the experiments reported in the main document.

1. Layer-wise Sparsity in *BasicNet*

In Section 2.3 and Table 2 in the main paper, we demonstrated that for BasicNet on CIFAR-100, Adam shows feature sparsity in both early layers and later layers, while SGD only shows sparsity in the early layers. We establish in the main paper that Adam learns selective features in the later layers which contribute to this additional sparsity. In Table 1 we show similar trends in layer-wise sparsity also emerge when trained on CIFAR-10.

Sparsity with AMSGrad: In Table 2 we compare the extent of sparsity of Adam with AMSGrad [27]. Given that AMSGrad tracks the long term history of squared gradients, we expect the effect of L2 regularization in the low gradient regime to be dampened, and for it to lead to less sparsity. For BasicNet, on CIFAR-100, with L2 regularization of 10^{-4} , AMSGrad only shows sparsity in the later layers, and overall only 13% of features are inactive. For a comparable test error for Adam, 47% of the features are inactive. In Table 4 we show the feature sparsity by activation and by γ for BasicNet with AMSGrad, Adamax and RMSProp, trained for CIFAR-10/100.

Sparsity with Leaky ReLU: Leaky ReLU is anecdotally [1] believed to address the ‘dying ReLU’ problem by preventing features from being inactivated. The cause of feature level sparsity is believed to be the accidental inactivation of features, which gradients from Leaky ReLU can help revive. We have however shown there are systemic processes underlying the emergence of feature level sparsity, and those would continue to persist even with Leaky ReLU. Though our original definition of feature selectivity does not apply here, it can be modified to make a distinction between data points which produce positive activations for a feature vs. the data points that produce a negative activation. For typical values of the negative slope (0.01 or 0.1) of Leaky ReLU, the more selective features (as per the updated definition) would continue to see lower gradients than the less selective features, and would consequently see relatively higher effect of regularization. For BasicNet trained

on CIFAR-100 with Adam, in Table 2 we see that using Leaky ReLU has a minor overall impact on the emergent sparsity.

2. On Feature Selectivity in Adam

In Figure 1, we show the the distribution of the scales (γ) and biases (β) of layers C6 and C5 of *BasicNet*, trained on CIFAR-100. We consider SGD and Adam, each with a low and high regularization value. For both C6 and C5, Adam learns exclusively negative biases and positive scales, which results in features having a higher degree of selectivity (i.e, activating for only small subsets of the training corpus). In case of SGD, a subset of features learns positive biases, indicating more universal (less selective) features.

Figure 2 shows feature selectivity also emerges in the later layers when trained on CIFAR-10, in agreement with the results presented for CIFAR-100 in Fig. 3 of the main paper.

Higher feature selectivity leads to parameters spending more iterations in a low gradient regime. In Figure 3, we show the effect of the coupling of L2 regularization with the update step of various adaptive gradient descent approaches in a low gradient regime. Adaptive gradient approaches exhibit strong regularization in low gradient regime even with low regularization values. This disproportionate action of the regularizer, combined with the propensity of certain adaptive gradient methods for learning selective features, results in a higher degree of feature level sparsity with adaptive approaches than vanilla SGD, or when using weight decay.

3. Effect of Other Hyperparameters on Sparsity

Having shown in the main paper and in Sec. 2 that feature selectivity results directly from negative bias (β) values when the scale values (γ) are positive, we investigate the effect of β initialization value on the resulting sparsity. As shown in Table 3 for BasicNet trained with Adam on CIFAR 100, a slightly negative initialization value of -0.1 does not affect the level of sparsity. However, a positive initialization value of 1.0 results in higher sparsity. This shows that attempting to address the emergent sparsity by changing the initialization of β may be counter productive.

We also investigate the effect of scaling down the learning rate of γ and β compared to that for the rest of the network (Table 3). Scaling down the learning rate of γ s by a factor of 10 results in a significant reduction of sparsity. This can likely be attributed to the decrease in effect of the L2 regularizer in the low gradient regime because it is directly scaled by the learning rate. This shows that tuning the learning of γ can be more effective than Leaky ReLU at controlling the emergent sparsity. On the other hand, scal-

ing down the learning rate of β s by a factor of 10 results in a slight increase in the extent of sparsity.

4. Experimental Details

For all experiments, the learned BatchNorm scales (γ) are initialized with a value of 1, and the biases (β) with a value of 0. The reported numbers for all experiments on CIFAR10/100 are averaged over 3 runs. Those on TinyImageNet are averaged over 2 runs, and for ImageNet the results are from 1 run. On CIFAR10/100, VGG-16 follows the same learning rate schedule as *BasicNet*, as detailed in Section 2.1 in the main paper.

On TinyImageNet, both VGG-16 and TinyImageNet follow similar schemes. Using a mini-batch size of 40, the gradient descent method specific base learning rate is used for 250 epochs, and scaled down by 10 for an additional 75 epochs and further scaled down by 10 for an additional 75

epochs, totaling 400 epochs. When the mini-batch size is adjusted, the number of epochs are appropriately adjusted to ensure the same number of iterations.

On ImageNet, the base learning rate for Adam is 1e-4. For *BasicNet*, with a mini-batch size of 64, the base learning rate is used for 15 epochs, scaled down by a factor of 10 for another 15 epochs, and further scaled down by a factor of 10 for 10 additional epochs, totaling 40 epochs. The epochs are adjusted with a changing mini-batch size. For VGG-11, with a mini-batch size of 60, the total epochs are 60, with learning rate transitions at epoch 30 and epoch 50. For VGG-16, mini-batch size of 40, the total number of epochs are 50, with learning rate transitions at epoch 20 and 40.

Table 1. Layerwise % filters pruned from BasicNet trained on CIFAR10, based on the $|\gamma| < 10^{-3}$ criteria. Also shown are pre-pruning and post-pruning test error, and the % of *convolutional* parameters pruned. C1-C7 indicate Convolution layer 1-7, and the numbers in parantheses indicate the total number of features per layer. Average of 3 runs. Also see Table 2 in the main document.

CIFAR10				% Sparsity by γ or % Filters Pruned								% Param		
		Train	Test	C1	C2	C3	C4	C5	C6	C7	Total	Pruned	Pruned	
		Loss	Loss											Err
Adam	L2: 1e-3	0.29	0.41	13.1	59	57	42	74	76	97	98	83	97	13.5
	L2: 1e-4	0.06	0.43	10.5	44	22	6	45	54	96	95	70	90	10.5
	WD: 2e-4	0.22	0.42	13.4	57	27	9	19	46	77	91	60	83	13.4
	WD: 1e-4	0.07	0.42	11.2	45	4	0	0	14	51	78	40	63	11.2
SGD	L2: 1e-3	0.62	0.64	21.8	86	61	53	46	65	4	0	27	38	21.8
	L2: 5e-4	0.38	0.49	16.3	68	16	9	9	24	0	0	9	13	16.5
	WD: 1e-3	0.61	0.63	21.6	85	60	51	46	66	4	0	27	38	21.6
	WD: 5e-4	0.38	0.46	15.8	69	19	7	7	23	0	0	8	13	16.1

Table 2. Layerwise % filters pruned from BasicNet trained on CIFAR100, based on the $|\gamma| < 10^{-3}$ criteria. Also shown are pre-pruning and post-pruning test error. C1-C7 indicate Convolution layer 1-7, and the numbers in parantheses indicate the total number of features per layer. Average of 3 runs.

Adam vs AMSGrad (ReLU)				% Sparsity by γ or % Filters Pruned								Pruned	
		Train	Test	C1	C2	C3	C4	C5	C6	C7	Total	Pruned	Pruned
		Loss	Loss										
Adam	L2: 1e-3	1.06	1.41	39.0	56	47	43	68	72	91	85	76	39.3
	L2: 1e-4	0.10	1.98	36.6	41	20	9	33	34	67	55	47	36.6
AMSGrad	L2: 1e-2	3.01	2.87	71.9	79	91	91	96	96	98	96	95	71.9
	L2: 1e-4	0.04	1.90	35.6	0	0	0	0	1	25	23	13	35.6
	L2: 1e-6	0.01	3.23	40.2	0	0	0	0	0	0	0	0	40.2

Adam With Leaky ReLU				% Sparsity by γ or % Filters Pruned								Pruned	
NegSlope=0.01		Train	Test	C1	C2	C3	C4	C5	C6	C7	Total	Pruned	Pruned
		Loss	Loss										
NegSlope=0.01	L2: 1e-3	1.07	1.41	39.1	49	40	39	62	61	81	85	70	39.4
	L2: 1e-4	0.10	1.99	36.8	33	20	9	31	29	55	53	41	36.8
NegSlope=0.1													
	L2: 1e-4	0.14	2.01	37.2	38	30	21	34	31	55	52	43	37.3

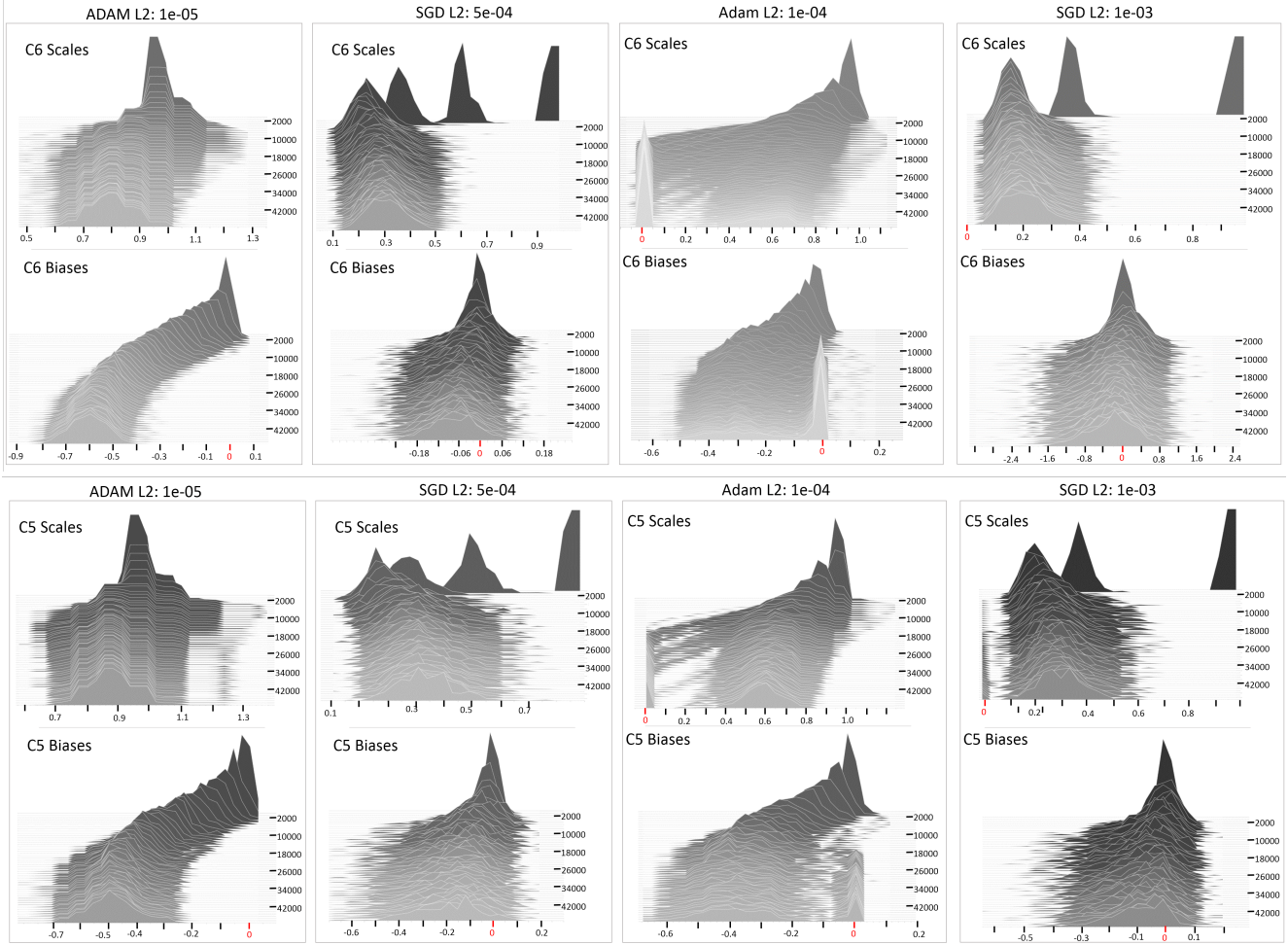


Figure 1. **Emergence of Feature Selectivity with Adam (Layer C6 and C5)** The evolution of the learned scales (γ , top row) and biases (β , bottom row) for layer C6 (top) and C5 (bottom) of *BasicNet* for Adam and SGD as training progresses, in both low and high L2 regularization regimes. Adam has distinctly negative biases, while SGD sees both positive and negative biases. For positive scale values, as seen for both Adam and SGD, this translates to greater feature selectivity in the case of Adam, which translates to a higher degree of sparsification when stronger regularization is used.

Table 3. Layerwise % filters pruned from *BasicNet* trained on CIFAR100, based on the $|\gamma| < 10^{-3}$ criteria. Also shown are pre-pruning and post-pruning test error. C1-C7 indicate Convolution layer 1-7, and the numbers in parantheses indicate the total number of features per layer. We analyse the effect of different initializations of β s, as well as the effect of different relative learning rates for γ s and β s, when trained with Adam with L2 regularization of 10^{-4} . Average of 3 runs.

	Train Loss	Test Loss	Test Err	% Sparsity by γ or % Filters Pruned								Pruned Test Err.
				C1 (64)	C2 (128)	C3 (128)	C4 (256)	C5 (256)	C6 (512)	C7 (512)	Total (1856)	
Baseline ($\gamma_{init}=1, \beta_{init}=0$)	0.10	1.98	36.6	41	20	9	33	34	67	55	46	36.6
$\gamma_{init}=1, \beta_{init}=-0.1$	0.10	1.98	37.2	44	20	10	34	32	68	54	46	36.5
$\gamma_{init}=1, \beta_{init}=1.0$	0.14	2.04	38.4	47	29	25	36	46	69	61	53	38.4
Different Learning Rate Scaling for β and γ												
LR scale for γ : 0.1	0.08	1.90	35.0	16	6	1	13	20	52	49	33	35.0
LR scale for β : 0.1	0.12	1.98	37.1	42	26	21	41	48	70	55	51	37.1

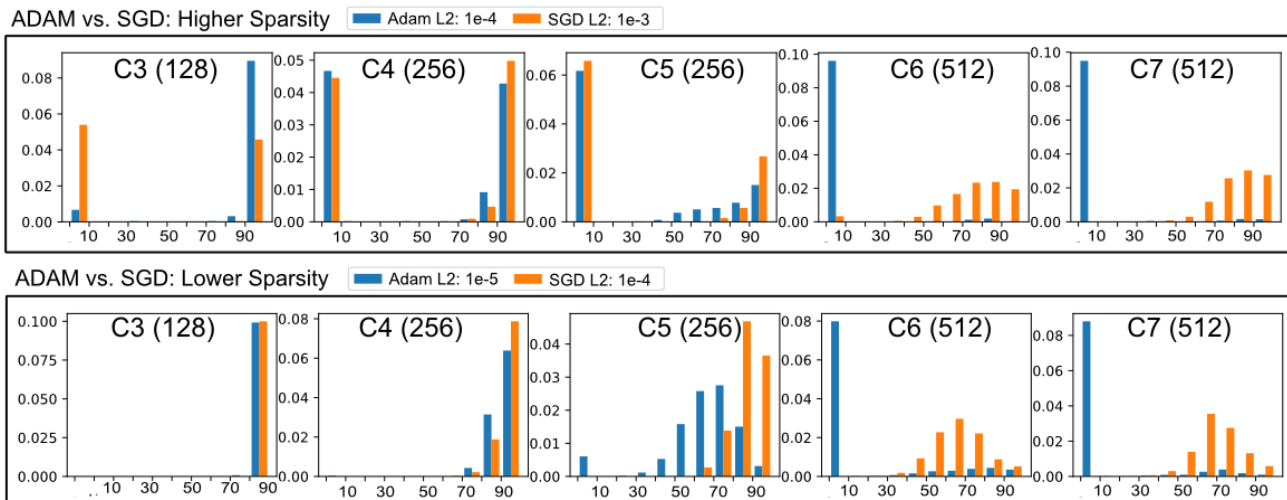


Figure 2. **Layer-wise Feature Selectivity** Feature universality for CIFAR 10, with Adam and SGD. X-axis shows the universality and Y-axis ($\times 10$) shows the fraction of features with that level of universality. For later layers, Adam tends to learn less universal features than SGD, which get pruned by the regularizer. Please be mindful of the differences in Y-axis scales between plots. Figure 3 in the main document shows similar plots for CIFAR100.

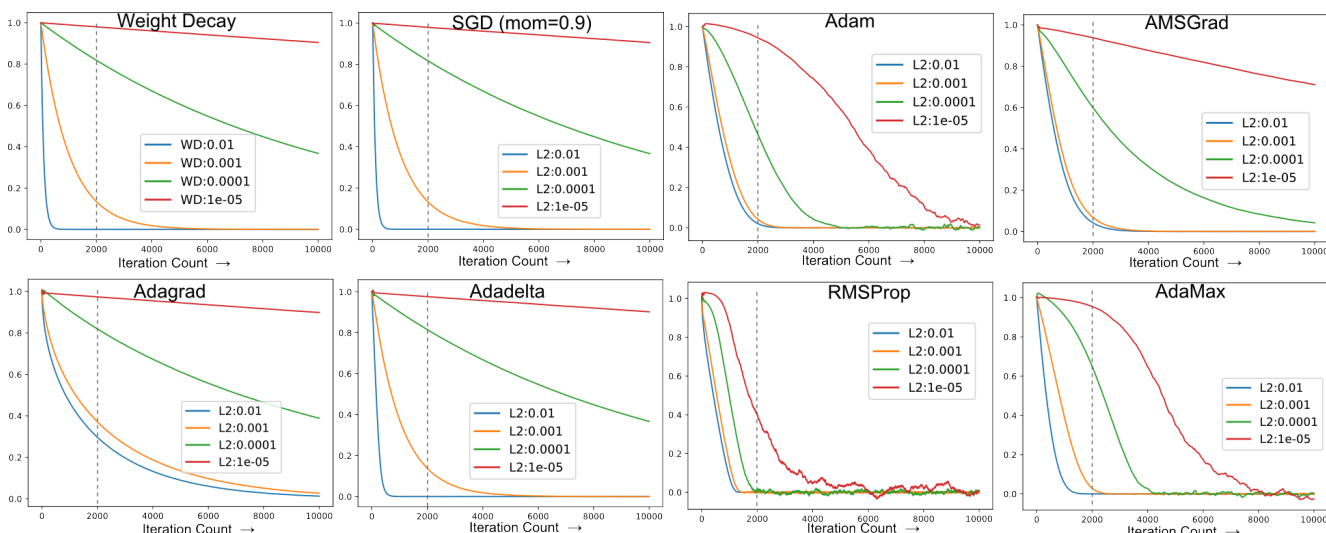


Figure 3. The action of regularization on a scalar value for a range of regularization values in the presence of simulated low gradients drawn from a mean=0, $\text{std}=10^{-5}$ normal distribution. The gradients for the first 100 iterations are drawn from a mean=0, $\text{std}=10^{-3}$ normal distribution to emulate a transition into low gradient regime rather than directly starting in the low gradient regime. The scalar is initialized with a value of 1. The learning rates are as follows: SGD(momentum=0.9,lr=0.1), ADAM(1e-3), AMSGrad(1e-3), Adagrad(1e-2), Adadelta(1.0), RMSProp(1e-3), AdaMax(2e-3). The action of the regularizer in low gradient regime is only one of the factors influencing sparsity. Different gradient descent flavours promote different levels of feature selectivity, which dictates the fraction of features that fall in the low gradient regime. Further, the optimizer and the mini-batch size affect together affect the duration different features spend in low gradient regime.

References

- [1] CS231n convolutional neural networks for visual recognition. <http://cs231n.github.io/neural-networks-1/>.
- [2] Tiny imagenet visual recognition challenge. <https://tiny-imagenet.herokuapp.com/>.
- [3] J. P. Cohen, H. Z. Lo, and W. Ding. Randomout: Using a convolutional gradient norm to rescue convolutional filters, 2016.
- [4] J. Deng, W. Dong, R. Socher, L.-J. Li, K. Li, and L. Fei-Fei. ImageNet: A Large-Scale Hierarchical Image Database. In *CVPR09*, 2009.
- [5] L. Dinh, R. Pascanu, S. Bengio, and Y. Bengio. Sharp minima can generalize for deep nets. In *ICML*, 2017.
- [6] J. Duchi, E. Hazan, and Y. Singer. Adaptive subgradi-

Table 4. Convolutional filter sparsity in *BasicNet* trained on CIFAR10/100 for Adamax, AMSGrad and RMSProp with L2 regularization. Shown are the % of non-useful / inactive convolution filters, as measured by activation over training corpus (max act. $< 10^{-12}$) and by the learned BatchNorm scale ($|\gamma| < 10^{-03}$), averaged over 3 runs. See Table 1 in main paper for other combinations of regularization and gradient descent methods.

	L2	CIFAR10			CIFAR100		
		% Sparsity	Test	Error	% Sparsity	Test	Error
		by Act	by γ		by Act	by γ	
AMSGrad	1e-02	93	93	20.9	95	95	71.9
	1e-04	51	47	9.9	20	13	35.6
	1e-06	0	0	11.2	0	0	40.2
Adamax	1e-02	75	90	16.4	74	87	51.8
	1e-04	49	50	10.1	10	10	39.3
	1e-06	4	4	11.3	0	0	39.8
RMSProp	1e-02	95	95	26.9	97	97	78.6
	1e-04	72	72	10.4	48	48	36.3
	1e-06	29	29	10.9	0	0	40.6

ent methods for online learning and stochastic optimization. *Journal of Machine Learning Research*, 12(Jul):2121–2159, 2011.

- [7] X. Glorot and Y. Bengio. Understanding the difficulty of training deep feedforward neural networks. In *Proceedings of the thirteenth international conference on artificial intelligence and statistics*, pages 249–256, 2010.
- [8] S. Han, H. Mao, and W. J. Dally. Deep compression: Compressing deep neural networks with pruning, trained quantization and huffman coding. In *ICLR*, 2016.
- [9] B. Hassibi, D. G. Stork, and G. J. Wolff. Optimal brain surgeon and general network pruning. In *Neural Networks, 1993., IEEE International Conference on*, pages 293–299. IEEE, 1993.
- [10] Y. He, J. Lin, Z. Liu, H. Wang, L.-J. Li, and S. Han. Amc: Automl for model compression and acceleration on mobile devices. In *Proceedings of the European Conference on Computer Vision (ECCV)*, pages 784–800, 2018.
- [11] H. Hu, R. Peng, Y.-W. Tai, and C.-K. Tang. Network trimming: A data-driven neuron pruning approach towards efficient deep architectures. *arXiv preprint arXiv:1607.03250*, 2016.
- [12] S. Ioffe and C. Szegedy. Batch normalization: Accelerating deep network training by reducing internal covariate shift. *arXiv preprint arXiv:1502.03167*, 2015.
- [13] N. S. Keskar, D. Mudigere, J. Nocedal, M. Smelyanskiy, and P. T. P. Tang. On large-batch training for deep learning: Generalization gap and sharp minima. In *ICLR*, 2017.
- [14] N. S. Keskar and R. Socher. Improving generalization performance by switching from adam to SGD. *arXiv preprint arXiv:1712.07628*, 2017.
- [15] D. P. Kingma and J. Ba. Adam: A method for stochastic optimization. *arXiv preprint arXiv:1412.6980*, 2014.
- [16] A. Krizhevsky and G. Hinton. Learning multiple layers of features from tiny images. 2009.
- [17] Y. LeCun, J. S. Denker, and S. A. Solla. Optimal brain damage. In *Advances in neural information processing systems*, pages 598–605, 1990.
- [18] H. Li, A. Kadav, I. Durdanovic, H. Samet, and H. P. Graf. Pruning filters for efficient convnets. In *ICLR*, 2017.
- [19] Z. Liu, J. Li, Z. Shen, G. Huang, S. Yan, and C. Zhang. Learning efficient convolutional networks through network slimming. In *Computer Vision (ICCV), 2017 IEEE International Conference on*, pages 2755–2763. IEEE, 2017.
- [20] Z. Liu, M. Sun, T. Zhou, G. Huang, and T. Darrell. Rethinking the value of network pruning. *arXiv preprint arXiv:1810.05270*, 2018.
- [21] I. Loshchilov and F. Hutter. Fixing weight decay regularization in adam. *arXiv preprint arXiv:1711.05101*, 2017.
- [22] A. L. Maas, A. Y. Hannun, and A. Y. Ng. Rectifier nonlinearities improve neural network acoustic models. In *Proc. icml*, volume 30, page 3, 2013.
- [23] P. Molchanov, S. Tyree, T. Karras, T. Aila, and J. Kautz. Pruning convolutional neural networks for resource efficient inference. 2017.
- [24] A. S. Morcos, D. G. Barrett, N. C. Rabinowitz, and M. Botvinick. On the importance of single directions for generalization. *arXiv preprint arXiv:1803.06959*, 2018.
- [25] M. C. Mozer and P. Smolensky. Skeletonization: A technique for trimming the fat from a network via relevance assessment. In *Advances in neural information processing systems*, pages 107–115, 1989.
- [26] A. Paszke, S. Gross, S. Chintala, G. Chanan, E. Yang, Z. DeVito, Z. Lin, A. Desmaison, L. Antiga, and A. Lerer. Automatic differentiation in pytorch. In *NIPS-W*, 2017.
- [27] S. J. Reddi, S. Kale, and S. Kumar. On the convergence of adam and beyond. In *ICLR*, 2018.
- [28] K. Simonyan and A. Zisserman. Very deep convolutional networks for large-scale image recognition. *arXiv preprint arXiv:1409.1556*, 2014.
- [29] S. Srinivas and R. V. Babu. Data-free parameter pruning for deep neural networks. In *BMVC*, 2016.
- [30] L. Theis, I. Korshunova, A. Tejani, and F. Huszár. Faster gaze prediction with dense networks and fisher pruning. In *ICLR*, 2017.
- [31] J. Ye, X. Lu, Z. Lin, and J. Z. Wang. Rethinking the smaller-norm-less-informative assumption in channel pruning of convolution layers. In *ICLR*, 2018.
- [32] M. D. Zeiler. Adadelta: an adaptive learning rate method. *arXiv preprint arXiv:1212.5701*, 2012.
- [33] B. Zhou, Y. Sun, D. Bau, and A. Torralba. Revisiting the importance of individual units in cnns via ablation. *arXiv preprint arXiv:1806.02891*, 2018.